ELSEVIER

Journal of Molecular Catalysis A: Chemical 119 (1997) 349–356

JOURNAL OF MOLECULAR CATALYSIS A: CHEMICAL

Mechanisms of silicon incorporation in aluminophosphate molecular sieves

G. Sastre, D.W. Lewis, C.R.A. Catlow *

Davy Faraday Research Laboratory, The Royal Institution of Great Britain, 21, Albemarle Street, WIX 4BS London, UK

Received 4 June 1996; accepted 8 July 1996

Abstract

The mechanisms of Si incorporation into aluminophosphate molecular sieves has been investigated using lattice simulation techniques. We consider the relative stability of dispersed Si and Si islands, along with changes in the substitution mechanisms in the different structure types. Two mechanisms are considered: P substitution by Si (SM2) and the replacement of adjacent Al and P with 2Si (SM3). We demonstrate that aggregation of silicon will only occur above certain thresholds determined by the structure type. Our previous work has demonstrated that silicon island formation by means of SM3 is energetically unfavourable, and thus 2Si and 4Si islands are not expected to form in SAPO structures. In contrast, the formation of silicon islands by means of a combination of SM2 and SM3 has proved to be energetically favourable, leading to 5Si and 8Si islands being stable in the SAPO structure. The instability of [Si–O–P] linkages is therefore demonstrated. We also investigate the stability of Si islands in a number of SAPO structures. We find differences in island stability in these different structures, which can be explained in terms of the connectivity of the framework structure.

Keywords: Silicon incorporation; Aluminophosphate; Molecular sieves; Aggregation; $AlPO_4$

1. Introduction

Crystalline alumino–phosphate molecular sieves of general formula $AlPO_4$ are formed by corner-sharing TO_4 tetrahedra (T = Al, P) producing [≡Al–O–P≡] unit with strict Al/P alternation [1]. Theoretically, an infinite number of microporous structures can be constructed from such tetrahedra and the frameworks synthesised so far have a very similar enthalpies of formation [2], suggesting that the synthesis is controlled by geometric and kinetic factors rather than energetic constraints. Therefore, the synthesis of new structures appears virtually limitless [2]. These materials are potentially exploitable in catalysis as a consequence of their microporous nature, with channels and cavities with dimensions in the range 5–15 Å, the same size of many organic molecules. However, the neutrality of the $AlPO_4$ framework drastically limits its catalytic applications due to the absence of cations and Brønsted acid sites, in contrast to aluminosilicates where the presence of Al provides the means to generate such sites. However, the incorporation of silicon into the framework will result in Brønsted acidity [3].

* Corresponding author.

PII S1381-1169(96)00498-0

The introduction of other elements into AlPO structures can also produce potentially active sites with medium to high acid strengths [4]. Consequently, the incorporation of other elements has been achieved forming a new family of materials, MeAPSOs (Me, metal). A wide range of compositional variants is possible with, for example, Co, Fe, Mg, Mn, Zn, Cr and Ti [5], a number of which have been found to be successful catalysts [6].

We will confine ourselves in this work to Si incorporation in the $AlPO_4$ framework owing to its importance in a wide range of catalytic processes. SAPO structures have been used as catalysts in industrial processes such as the conversion of light olefins to gasoline-range products, catalytic reforming of naphthenes and the isomerisation of C_8 aromatics [7]. The key physical property of this catalytic behaviour is the acidity of the SAPO structure. SAPO materials in the protonic form often show mild acidity, the Brønsted sites in these materials being formed by the substitution of P by Si [8], again in contrast to aluminosilicates which exhibit stronger Brønsted acidity [9]. Increasing the amount of silicon in the framework of the SAPO materials can lead to high acidity in certain acid-catalysed reactions [10] and therefore it is advantageous to synthesise SAPOs with the highest possible silicon content. Likewise, for applications where medium-strength acidity is required, it is desirable to control the synthesis conditions to favour the formation of such sites. A particularly interesting feature of silicon incorporation in AlPOs is the formation of silicon islands, i.e. aggregates where at least two adjacent T sites are substituted by silicon. The formation of these islands has been established by ^{29}Si NMR experiments [11]. When high acidity is required, the formation of silicon islands in the structure must be maximised since the acid centres at the border of these islands posses higher acid strength than those of dispersed silicon [12]. The equilibrium between the silicon present as islands and the dispersed silicon determines the catalytic properties of the SAPO.

We have found previously that energetic factors play an important role in explaining the silicon distribution throughout the framework [13]. Our results, moreover, allow us to characterise the local deformations arising from the silicon substitution. We concentrate here on SAPO-5 and SAPO-34, for which there is a considerable amount of information regarding silicon distributions with which we can compare our theoretical results [14]. Additional calculations focusing on silicon distributions at low silicon content have also been performed in SAPO-11, SAPO-18, and SAPO-31. Overall, our work leads to an improved understanding of both particular and general features of silicon incorporation in SAPOs and the role of the Si distribution influencing their acidity.

2. Methodology

The methodologies are based on the use of static lattice minimisation methods based on interatomic potentials. The GULP code [15] is used for all the calculations reported in the paper. Summation of the long-range Coulombic interactions employed the Ewald [16] method, while direct summation is used for the short-range interactions with a cutoff distance of 10 Å. Formal charges were considered for the atoms of the framework. As discussed elsewhere [13], the interatomic potentials modelling the interactions between the atoms in the structure included Coulombic, short-range Buckingham and three-body bond-bending terms with a shell model [17] representation of the polarisability of the oxygen atoms. The Mott–Littleton methodology [18] was employed to treat the incorporation of defects within the perfect lattice. These methods and potentials have previously been shown to successfully model both zeolites [19], AlPOs [20] and recently we have applied them to the study of SAPOs [13]. Further details of the methodology and a full list of potential parameters are given in reference [13].

3. Models

Si can be introduced into the AlPO structure by two substitution mechanisms:

$$\text{SM2: } [\overset{\text{AlPO framework}}{AlPO_4}] + Si^{4+} + H^+ \rightarrow [\overset{\text{SAPO framework}}{Si, H}]_P + P^{5+} \quad (1)$$

$$\text{SM3: } [AlPO_4] + 2Si^{4+} \rightarrow [2Si]_{Al,P} + P^{5+} + Al^{3+} \quad (2)$$

The notation employed shows the species present in the final (in square brackets) and initial structures (in sub indexes). The energies involved in these equations are defect energies, i.e. the energy necessary to introduce and extract the ions cations in and out the structure and no consideration is given to the source or the sink of the cations involved — see Ref. [13] for a fuller treatment.

The formation of 5Si and 8Si islands can be described as a combination of the two previous mechanisms as follows:

$$\text{5Si island: } [AlPO_4] + 5Si^{4+} + 3H^+ \rightarrow [5Si, 3H]_{Al,4P} + 4P^{5+} + Al^{5+} \quad (3)$$

$$\text{8Si island: } [AlPO_4] + 8Si^{4+} + 4H^+ \rightarrow [8Si, 4H]_{2Al,6P} + 6P^{5+} + 2Al^{5+} \quad (4)$$

4. Results and discussion

We consider first the formation of a single Brønsted acid site, in both $AlPO_4$-5 and $AlPO_4$-34, through the SM2 mechanism (Eq. (1)) and investigate the role of both short and long-range interactions on the resulting substituted framework. We note that pure $AlPO_4$-34 has not been prepared; this structural type exists only as a SAPO or MeAPO, a consequence of the need for high template concentration to form the structure [21]. The defect energies presented (Table 1) include only the energy change on bringing the substituent from infinity, and displacing the substituents from the framework to infinity and do not therefore represent a thermodynamic cycle [13,22]. However, the differences in energy will be an accurate measure of any differences between the systems. The results of the calculations (Table 1) show a range of energies varying by 0.28 eV in $AlPO_4$-5 and 0.21 eV in $AlPO_4$-34 between the different oxygen sites which are protonated. These differences may be related to the existence of centres of different acid strength observed experimentally [23]. However, it can be seen that the differences in the defect energy in the two structures are rather small and thus this mechanism of substitution appears to be independent of the framework structure considered.

Table 1
Defect energies (eV) for the silicon incorporation according to the SM2 mechanism, P → Si, H, in $AlPO_4$-5 and $AlPO_4$-34

	$AlPO_4$-5	$AlPO_4$-34
$E_{\text{Si-disp}}$(O1)	59.06	58.94
$E_{\text{Si-disp}}$(O2)	59.15	59.09
$E_{\text{Si-disp}}$(O3)	58.87	59.13
$E_{\text{Si-disp}}$(O4)	58.90	58.92

An analysis of the geometries of the local acid site has been performed to determine the effect of the substitution on the environment of the framework. Two examples will be discussed: the PO4Al → SiO4(H)Al in $AlPO_4$-5, and the PO2Al → SiO2(H)Al in $AlPO_4$-34 (Table 2). The geometry of the local neighbours of the acid sites changes considerably as a consequence of the new [Si–O–Al] linkages. However, the geometry in the next nearest neighbours remains practically unchanged. Therefore, we conclude that the effect of silicon incorporation into the framework (by the SM2 mechanism) affects only the first neighbours of a substituted P atom.

Calculations have also been performed on the electrostatic potential at the T-sites in both AlPO structures [24] to estimate the long range contribution to the substitution energy. A formal charge model is used with the Ewald summation being employed. These results show similar po-

Table 2
Geometries of the first neighbors after silicon incorporation according to the SM2 mechanism, P → Si, H, in $AlPO_4$-5 and $AlPO_4$-34

	T–O (Å)	O–Al(Å)	TO(H)Al(°)
$AlPO_4$-5 (T = P)	1.52	1.72	149.0
SAPO-5 (T = Si)	1.78	1.82	136.9
$AlPO_4$-34 (T = P)	1.51	1.73	142.8
SAPO4-34 (T = Si)	1.77	1.82	138.4

tentials for both the structures, supporting our argument that, the differences in the defect energies are largely due to structural changes in the proximity of the acid centre. This result also suggests that silicon incorporation by the SM2 mechanism will occur with equal probability regardless of the AlPO structure considered, if such a substitution is controlled by energetic considerations.

In addition to the isolated Brønsted sites considered above, silicon islands are also known to form in SAPOs. Whilst the formation of isolated Brønsted sites takes place through SM2 (Eq. (1)) the formation of silicon islands takes place by means of a combination of SM2 and SM3 (Eqs. (3) and (4)). The relative extent of these two mechanism will determine the number and distribution of Brønsted acid sites in the resulting SAPO structure. The structures of SAPO-5 and SAPO-34 appear to behave differently as the silicon distribution increases in the structure [25]. It has been observed that in SAPO-34 the silicon islands form after a silicon content of 18% is reached, while in SAPO-5 the silicon islands are observed once a silicon content of 10% is attained [26]. There appear therefore to be structural dependent are factors controlling Si island formation. As a consequence, the mechanism of Si substitution will have a considerable effect on the catalytic behaviour of both structures. In order to achieve a better understanding of the process of Si island formation we have performed calculations aimed at accounting for the distribution of Brønsted sites and silicon islands at low silicon content.

It has been proposed that before silicon islands are observed, smaller aggregates of Si may exist in the framework [26]. We have previously shown that isolated 2Si aggregates are unstable with respect to isolated Brønsted acid sites [13].

Another type of small aggregate is a cluster of 3 Brønsted acid sites, which can be considered as a precursor to a 5Si island (Fig. 1). The relative stability of these aggregates can be compared with two other possible distributions: the three Brønsted sites at infinite distance, and an aggregate of the type –Si–Al–Si– with the third acid site at an infinite distance from this 2Si aggregate. We have calculated the energy of these different distributions of three Brønsted sites and the relative difference in energy between them will give us an estimate of the preferred silicon distribution. The calculations have been carried out in both SAPO-5 and SAPO-34 and the results (Table 3) show that the conformations containing Al(3Si, 1P) are higher in energy in both structures. We note that although the differences in energy are not very high (particularly in the case of SAPO-34), an additional entropic term (not included in these calculations) will also favour the formation of more dispersed configurations, meaning that the formation of the Al(3Si, 1P) aggregate will only occur if the silicon content reaches a level such that isolated silicon (–Si–Al–P–Al–Si–) can

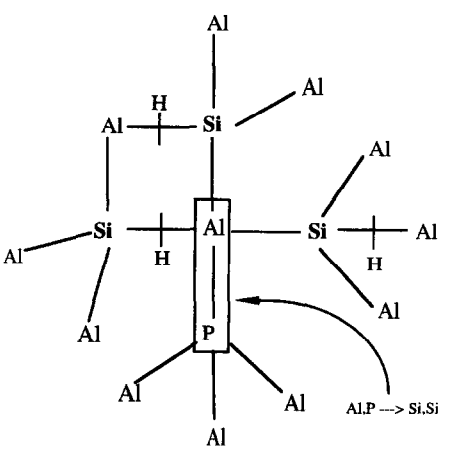

Fig. 1. Mechanism of formation of 5Si islands in SAPO-5 through mechanisms SM2 + SM3 (Eqs. (1) and (2)).

Table 3
Defect energies (eV) for the incorporation of 3Si according to SM2 (P → Si, H) in $AlPO_4$-5 and $AlPO_4$-34. See text for a description of the configurations considered

Conformation	$AlPO_4$-5	$AlPO_4$-34
Al(3Si, 1P)	177.74	177.31
–Si–Al–Si–...–Si [a]	177.30	177.17
–Si–...–Si–...–Si– [b]	177.45	177.27

[a] One of the silicons is at infinite distance of an aggregate –Si–Al–Si.
[b] The three silicons are at infinite distance of each other.

no longer exist. The maximum silicon content at which isolated silicon can no longer form can be calculated from the topology of the framework using the 'topological density concept' developed by Barthomeuf [27] which gives maximum silicon contents of 9.0% and 10.8% in SAPO-5 and SAPO-34 respectively, which is in agreement with ^{29}Si NMR results [25]. Consequently, if the formation of Si islands leads to more stable configurations than Al(3Si, 1P) clusters, then island formation will dominate at higher Si concentrations.

We now consider the formation of silicon islands in SAPOs. Experimentally it is noted that islands with relatively small amount of Si dominate the structure of SAPOs and we have therefore modelled 5Si and 8Si islands. The stability of these aggregates with respect to silicon distributions containing [Si–O–P] linkages has already been shown in SAPO-5 [13], demonstrating the energetic penalty for forming such bonds. Here, we will focus on the differences in the formation energies of these silicon islands due to different framework topologies by considering SAPO-5 and SAPO-34. The formation of 5Si and 8Si islands take place as described in Eqs. (3) and (4) and the resulting islands are illustrated in Fig. 2. The results (Table 4) show a very similar defect energy for the formation of 5Si islands in both SAPO-5 and SAPO-34. However, there is a significant difference in the energy required to form an 8Si island in the two structures, with the 8Si structure being less stable in SAPO-34. This result

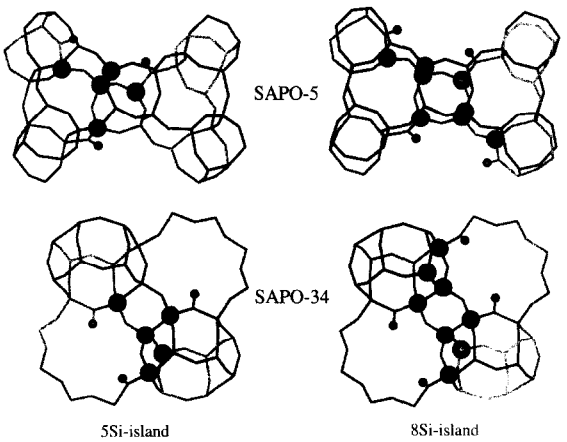

Fig. 2. 5Si islands and 8Si islands in SAPO-5 and SAPO-34.

may well explain the experimental observation of the earlier appearance of silicon islands in SAPO-5 than in SAPO-34.

The differences in the formation energy of the 8Si island can be explained by considering the different skeletal deformations allowed in both structures, particularly of the 4-T windows. For an 8Si island to be formed the four atoms in the 4-T ring must be substituted by silicon. The substitutions result in distortion of the geometry of the ring which are accommodated to different degrees in the two structures as a consequence of the topological flexibility of the structures. It is easier for the framework to absorb the deformations when the 4-T rings are connected to other larger windows. The 4-T windows are connected to other 4-T windows and to an 8-T window in SAPO-34 and to 6-T and 12-T windows in SAPO-5. We therefore conclude that, the more rigid units surrounding the 4-Si ring in SAPO-34 cannot absorb the deformations resulting from this level of silicon incorporation. Consequently, the energy required to form the

Table 4
Defect energies (eV) corresponding to the formation of 5Si and 8Si islands in SAPO-5 and SAPO-34. See Fig. 2

	SAPO-5	SAPO-34
$E_{5Si\text{-}isl}$	188.46	188.42
$E_{8Si\text{-}isl}$	258.13	259.39

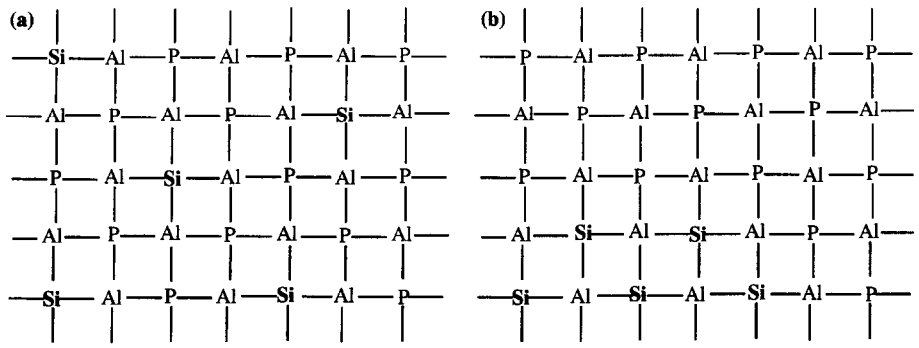

Fig. 3. Two different Si distributions in SAPOs. (a) The Si atoms are dispersed forming P–Al–Si–Al–P units. (b) The silicon atoms are clustered forming an aluminosilicate phase.

8Si island is higher than in SAPO-5. There is therefore an important contribution related to the structure of the framework and the connectivity of different rings which substantially influences the formation of certain types of silicon islands. Although the formation of silicon islands takes place in the gel-phase, before the long range structure has been determined, these silicon islands must still be compatible with the structure of the crystalline material formed. The calculated differences in energy of the 8Si islands in the two structures are therefore a major factor in controlling the extent of island formation in the two structures.

Finally, we consider the influence of long range silicon ordering on the stability of some SAPO structures. For this purpose, SAPO-11, SAPO-18 and SAPO-31 have been studied. The results discussed above have already shown a tendency to avoid the formation of Al(3Si, 1P) (a cluster of 3 Brønsted acid sites) unless the Si content is such that these configurations cannot be avoided. We can consider this effect as the result of the strains imposed on the framework as a consequence of positioning three (P → Si, H) substitutions close to each other (Fig. 1). The calculations performed now are aimed at modelling this effect in a more realistic way by considering periodic silicon distributions. Two different distributions were considered in each SAPO. In the first distribution (Fig. 3a) all the silicons are of the type Si(4Al)(nP) where n is the number of next nearest neighbours of the central Si atom. This type of silicon distribution has been observed in some SAPO structures, particularly in SAPO-37 [28], and its existence

Table 5
Energies (eV) corresponding to the formation of 'dispersed Si', single silicon substitution, aluminophosphate, and 'aluminosilicate phase' [a] in SAPO-11, SAPO-18, and SAPO-31

	SAPO-11	SAPO-18	SAPO-31
Stoichiometry	$P_{40}Al_{40}O_{160}$	$P_{48}Al_{48}O_{192}$	$P_{36}Al_{36}O_{144}$
E_{alpo}	−10722.97	−12862.15	−9651.75
Stoichiometry	$Si_1P_{39}Al_{40}O_{160}H_1$	$Si_1P_{47}Al_{48}O_{192}H_1$	$Si_1P_{35}Al_{36}O_{144}H_1$
$E_{single\text{-}Si}$	59.20	59.10	59.07
Stoichiometry	$Si_8P_{32}Al_{40}O_{160}H_8$	$Si_6P_{42}Al_{48}O_{192}H_6$	$Si_6P_{30}Al_{36}O_{144}H_6$
$E_{dispersed\text{-}Si}$	−10250.97	−12507.78	−9297.12
$E_{aluminosilicate}$	−10250.56	−12507.68	−9296.97
$\Delta E_{(dispSi\text{-}alsi)}$	−0.41	−0.10	−0.15
$(E_{dispSi} - E_{alpo})/n$ [b]	59.00	59.06	59.11

[a] See Fig. 3 for 'dispersed-Si' and 'aluminosilicate phase' distributions.
[b] n = number of silicon atoms introduced in the framework. $n = 8$ (SAPO-11), $n = 6$ (SAPO-18 and SAPO-31).

strongly supports the idea that silicon islands are avoided at low silicon contents. In the second distribution (Fig. 3b) a maximum number of [Si–Al–Si] linkages are created; the resulting structure resembles a zeolitic structure in the sense that there is a considerable region of an aluminosilicate phase. Again this distribution is experimentally observed [9]. It can be seen that the silicon content in both cases is the same, but the *distribution* is different. The interpretation of experimental data is sometimes difficult and both these distributions can fit the observations [26,29]. The results (Table 5) show the different silicon contents present in each structure and the relative energy necessary to pass from the 'dispersed silicon' distribution to the 'aluminosilicate phase' distribution. It can be seen that in the three cases studied, SAPO-11, SAPO-18 and SAPO-31, the lowest energy corresponds to the 'dispersed silicon' distribution. The differences are rather small (0.10 and 0.15 eV) in SAPO-18 and SAPO-31, but higher (0.41 eV) in SAPO-11. There is therefore a structure-dependent factor influencing the relative stability of both distributions and different occurrences of these distributions can be expected in different structures. Furthermore, we can expect entropic effects to further stabilise dispersed distributions. We also calculated the energy required to introduce a single silicon atom into the same unit cells (Table 5) which results allow us to compare the relative stability of 'dispersed' and 'aluminosilicate' phases with more dilute substitutions. If we compare the average energy of substitution of each silicon in the 'dispersed' phase ($E_{\text{dispersed-Si}}/n_{\text{Si}}$; $n = 8$ in SAPO-11, $n = 6$ in SAPO-18 and SAPO-31 with n_{Si} = number of silicon atoms) with the energy to introduce a single silicon atom (E_{Si}), it can be seen that there is little difference. This result further supports our previous conclusions that framework deformation on Si substitution is restricted to the nearest neighbours of the Si and thus the 'dispersed' phase can be considered as an aggregate of isolated Si in terms of the energetic changes resulting from its formation.

5. Conclusions

Defect energies for the process of single silicon incorporation according to SM2 (P → Si, H) have been calculated in SAPO-5 and SAPO-34. We find that the process appears to be independent of the framework type considered, since the distortion to the framework is limited to the first neighbours of the replaced P atom.

Aggregates of three acid centres containing Al(3Si, 1P) are found to be unstable with respect to more disperse configuration in both SAPO-5 and SAPO-34. Therefore such configurations are unlikely to form unless the silicon content is such that it is no longer possible to form isolated silicon (–Si–Al–P–Al–Si–) in the structure.

When we consider the formation of silicon islands in SAPO-5 and SAPO-34 we find that there is a structure-dependence on the formation energy of 8Si islands. These differences have been explained in terms of the medium-range flexibility of the framework. The smaller 5Si island however, have a similar energy in both structures. These findings can explain the different occurrence of silicon islands and hence the silicon distribution at a given silicon content.

Finally, we considered the effect of long range silicon ordering in SAPO-11, SAPO-18 and SAPO-31. We find that 'dispersed silicon' is more stable than a distribution which has large areas of an 'aluminosilicate phase'. Again we find differences which are dependent on the topology of the framework. However, these differences are quite small and therefore we would expect that, given suitable control of the synthesis conditions, both types of distribution are possible in these SAPO materials.

In this paper, we have shown how calculations on the incorporation of Si into aluminophosphate molecular sieves can provide insights into the formation of different Si distributions in these materials. Such information in turn can be used to understand further the catalytic properties of these materials. Future work will consider the different acidity arising from

the different substitution mechanisms and the actual process of Si incorporation in the gel medium.

Acknowledgements

We acknowledge financial support from MEC (Spain) and EPSRC (UK). We are also grateful to MSI for the provision of the InsightII software.

References

[1] C.S. Blackwell and R.L. Patton, J. Phys. Chem. 92 (1988) 3965.
[2] A. Navrotsky, I. Petrovic, Y. Hu, C-Y. Chen and M.E. Davis, Microporous Mater. 4 (1995) 95.
[3] E.M. Flanigen, R.L. Patton and S.T. Wilson, in: P.J. Grobet et al. (Eds.), Innovation in Zeolite Material Science, Stud. Surf. Sci. Catal. 37 (1988) 13.
[4] M.A. Asensi, A. Corma and A. Martinez, J. Catal. 158 (1996) 561.
[5] E.M. Flanigen, B.M. Lok, R.L. Patton and S.T. Wilson, in: Y. Murakami, A. Iijima and J.W. Ward (Eds.), New Developments in Zeolite, Science and Technology (Elsevier, N.Y., 1986) p. 103.
[6] P.R. Pujado, J.A. Rabo, G.J. Antos and S.A. Genbicki, Catal. Today 13 (1992) 113.
[7] L.H. Gielgens, I.H.E. Veenstra, V. Ponec, M.J. Haanepen and J.H.C. van Hoof, Catal. Lett. 32 (1995) 195.
[8] M. Mertens, J.A. Martens, P.J. Grobet and P.A. Jacobs, in: D. Barthomeuf, E.G. Derouane and W. Holderich (Eds.), Guidelines for Mastering the Properties of Molecular Sieves, NATO ASI Series B, Vol. 221 (Plenum Press, New York, 1990) p. 1.
[9] J.A. Rabo and G.A. Gajda, Catal. Rev. Sci. Eng. 31 (1989) 385.
[10] B. Zibrowius, E. Loffler and M. Hunger, Zeolites 12 (1992) 167.
[11] D. Freude, H. Ernst, M. Hunger, H. Pfeifer and E. Jahn, Chem. Phys. Lett. 143 (1988) 477.
[12] M. Briend, M. Derewinski, A. Lamy and D. Barthomeuf, in: L. Guczi, F. Solymosi and P. Tetenyi (Eds.), New Frontiers in Catalysis, 10th Int. Congr. Catal., Akademiai Kiado, Budapest, Hungary (1993) p. 409.
[13] G. Sastre, D.W. Lewis and C.R.A. Catlow, J. Phys. Chem. 100 (1996) 6722.
[14] E.M. Flanigen, B.M. Lok, R.L. Patton and S.T. Wilson, in: Y. Murakami, A. Iijima and J.W. Ward (Eds.), New Developments in Zeolite Science and Technology (Elsevier, N.Y., 1986) p. 103.
[15] J.D. Gale, General Utility Lattice Program (GULP), The Royal Institution of Great Britain/Imperial College (1992–1996).
[16] P.P. Ewald, Ann. Phys. 64 (1921) 253.
[17] B.G. Dick and A.W. Overhauser, Phys. Rev. 112 (1958) 90.
[18] N.F. Mott and M.J. Littleton, Trans. Faraday Soc. 34 (1938) 485.
[19] C.R.A. Catlow (Ed.), in: Modelling of Structure and Reactivity in Zeolites (Academic Press, London, 1992).
[20] J.D. Gale and N.J. Henson, J. Chem. Soc. Faraday Trans. 90 (1994) 3175.
[21] D.W. Lewis, C.R.A. Catlow and J.M. Thomas, Chem. Mater. 8 (1996) 1112.
[22] S.I. Zones, Eur. Pat. Appl. 231019 (1987).
[23] L. Smith, A.K. Cheetham, R.E. Morris, L. Marchese, J.M. Thomas, P.A. Wright and J. Chen, Science 271 (1996) 799.
[24] G. Sastre, D.W. Lewis and C.R.A. Catlow, submitted for publication.
[25] D. Barthomeuf, in: J. Fraissard and L. Petrakis (Eds.), Acidity and Basicity in Solids. Theory, Assessment and Utility, NATO ASI Series C, Vol. 444 (1993) p. 375.
[26] A.F. Ojo, J. Dwyer, J. Dewing, P.J. O'Malley and A. Nabhan, J. Chem. Soc. Faraday Trans. 88 (1992) 105.
[27] D. Barthomeuf, J. Phys. Chem. 97 (1993) 10092.
[28] L. Sierra de Saldarriaga, C. Saldarriaga and M. Davis, J. Am. Chem. Soc. 109 (1987) 2686.
[29] J.A. Martens, P.J. Grobet and P.A.J. Jacobs, Catal. 126 (1990) 299.